FERONIA interacts with ABI2-type phosphatases to facilitate signaling cross-talk between abscisic acid and RALF peptide in *Arabidopsis*

Jia Chen[a,b,1], Feng Yu[a,b,1,2], Ying Liu[a], Changqing Du[a], Xiushan Li[a], Sirui Zhu[a], Xianchun Wang[b], Wenzhi Lan[c], Pedro L. Rodriguez[d], Xuanming Liu[a], Dongping Li[b], Liangbi Chen[b], and Sheng Luan[e,2]

[a]Hunan Province Key Laboratory of Plant Functional Genomics and Developmental Regulation, Hunan University, Changsha 410082, People's Republic of China; [b]College of Life Sciences, Hunan Normal University, Changsha 410081, People's Republic of China; [c]Nanjing University–Nanjing Forestry University (NJU-NJFU) Joint Institute for Plant Molecular Biology, School of Life Sciences, Nanjing University, Nanjing 210093, People's Republic of China; [d]Instituto de Biología Molecular y Celular de Plantas, Consejo Superior de Investigaciones Científicas–Universidad Politécnica de Valencia, 46022 Valencia, Spain; and [e]Department of Plant and Microbial Biology, University of California, Berkeley, CA 94720

Edited by Steven P. Briggs, University of California, San Diego, La Jolla, CA, and approved July 19, 2016 (received for review May 27, 2016)

Receptor-like kinase FERONIA (FER) plays a crucial role in plant response to small molecule hormones [e.g., auxin and abscisic acid (ABA)] and peptide signals [e.g., rapid alkalinization factor (RALF)]. It remains unknown how FER integrates these different signaling events in the control of cell growth and stress responses. Under stress conditions, increased levels of ABA will inhibit cell elongation in the roots. In our previous work, we have shown that FER, through activation of the guanine nucleotide exchange factor 1 (GEF1)/4/10-Rho of Plant 11 (ROP11) pathway, enhances the activity of the phosphatase ABA Insensitive 2 (ABI2), a negative regulator of ABA signaling, thereby inhibiting ABA response. In this study, we found that both RALF and ABA activated FER by increasing the phosphorylation level of FER. The FER loss-of-function mutant displayed strong hypersensitivity to both ABA and abiotic stresses such as salt and cold conditions, indicating that FER plays a key role in ABA and stress responses. We further showed that ABI2 directly interacted with and dephosphorylated FER, leading to inhibition of FER activity. Several other ABI2-like phosphatases also function in this pathway, and ABA-dependent FER activation required PYRABACTIN RESISTANCE (PYR)/PYR1-LIKE (PYL)/REGULATORY COMPONENTS OF ABA RECEPTORS (RCAR)–A-type protein phosphatase type 2C (PP2CA) modules. Furthermore, suppression of *RALF1* gene expression, similar to disruption of the *FER* gene, rendered plants hypersensitive to ABA. These results formulated a mechanism for ABA activation of FER and for cross-talk between ABA and peptide hormone RALF in the control of plant growth and responses to stress signals.

signal transduction | root growth | plant hormones

Plants are constantly bombarded with environmental signals, and they must integrate these cues into plant growth control to adapt to the changing environment. The phytohormone ABA plays a central role in these responses (1–3). Plant ABA content increases under drought or salinity stress conditions, inducing guard cell closure and accumulation of osmo-compatible solutes and stress response gene expression, thus enhancing the capacity to cope with stress conditions (1–3). Given the importance of ABA to plant responses to environmental stress conditions, understanding the signal transduction processes linking the hormone to target responses has been a focus of abiotic stress research.

The discovery of the PYRABACTIN RESISTANCE (PYR)/PYR1-LIKE (PYL)/REGULATORY COMPONENTS OF ABA RECEPTORS (RCAR) proteins as a family of ABA receptors and the biochemical pathway leading receptors to downstream components represents a major breakthrough in plant stress responses. In this pathway, a key negative regulatory step is mediated by a group of protein phosphatases called A-type protein phosphatase type 2Cs (PP2Cs) that, in the absence (or presence of low levels) of ABA, interact with and inhibit the activity of several SnRK2-type protein kinases, critical positive regulators in the pathway. When ABA levels in plants increase, it will induce the formation of a protein complex consisting of PYR/PYL/RCAR receptor proteins interacting with A-type PP2Cs, and thus inhibit the phosphatase activity of PP2Cs and release the SnRK2 kinases in their active forms to trigger downstream events (1–3). These downstream processes include stomatal closure, activation of ABA response genes, and cell growth inhibition through repression of AHA2-mediated acidification of extracellular medium (1-4). In all these signaling processes, the A-type PP2Cs serve as coreceptors of ABA, and their activity represents an on–off switch in control of ABA responses.

Receptor-like protein kinases (RLKs) contain an extracellular receptor domain and a Ser/Thr kinase domain and are often localized at the plasma membrane and play critical roles in transduction of various environmental and developmental signals (5). FERONIA (FER), an RLK member in the *Cr*RLK subfamily in *Arabidopsis* (6–8), has been initially shown to function in fertilization (9). Recent reports further show that FER controls pollen tube rupture during fertilization through regulating calcium mobilization (10, 11). Duan et al. (10) showed that FER controls the production of high levels of reactive oxygen species (ROS) at the entrance to the female gametophyte/synergid cell through a NADPH reductase, and high ROS will induce pollen tube rupture in a calcium-dependent manner. Ngo et al. (11) also found that

Significance

Receptor-like kinase FERONIA (FER) not only serves as a receptor for growth-regulating rapid alkalinization factor (RALF) peptide but also acts as an important node in a variety of other signaling pathways, including plant responses to hormones, pathogens, and abiotic stresses. However, the mechanism underlying FER actions in these signaling cross-talks remain largely unknown. Our previous work identified a molecular relay that allows FER to inhibit abscisic acid (ABA) response through activation of a small G protein to enhance the activity of the clade A protein phosphatase type 2C (PP2C) ABA Insensitive 2 (ABI2), a repressor of ABA response. In this study, we found that ABI2 can directly interact and dephosphorylate FER, providing a feedback mechanism for RALF activation of FER.

Author contributions: F.Y. and S.L. conceived the project; F.Y. and S.L. designed research; J.C., F.Y., Y.L., C.Q.D., X.S.L., S.R.Z., X.C.W., and W.Z.L. performed research; P.L.R., X.M.L., D.P.L., and L.B.C. contributed new reagents/analytic tools; J.C., F.Y., and S.L. analyzed data; and J.C., F.Y., and S.L. wrote the paper.

The authors declare no conflict of interest.

This article is a PNAS Direct Submission.

[1]J.C. and F.Y. contributed equally to this work.

[2]To whom correspondence may be addressed. Email: sluan@berkeley.edu or feng_yu@hnu.edu.cn.

This article contains supporting information online at www.pnas.org/lookup/suppl/doi:10.1073/pnas.1608449113/-/DCSupplemental.

FER is required for the generation of calcium spikes both in the pollen tube and in synergid cells at the stage of pollen tube rupture.

Work by Haruta et al. (12) shows that FER serves as a receptor for a peptide hormone called rapid alkalinization factor (RALF). Interestingly, FER is also required for RALF-induced calcium spikes that further produce an inhibitory effect on root growth. Studies have also identified function of FER in other growth control processes, such as suppression of integument cell elongation, and thus seed size (13). However, FER can also promote cell growth through integrating different hormone signaling pathways (14, 15). For example, Duan et al. (14) showed that FER activates the guanine nucleotide exchange factor (GEF)-plant RHO GTPase (ROP/ARAC) pathway to produce ROS required for root hair growth. In the other case, *FER* expression is up-regulated by brassinosteroid (BR) and positively regulates BR-mediated response (15). In addition to these two hormones (auxin and BR) that typically play a positive role in cell growth, FER also suppresses ethylene and ABA response, two hormones that often have negative role in cell growth (16, 17).

Taken together, FER acts as a versatile regulator that controls cell growth differently in distinct cell types and in response to different environmental cues. It is intriguing how FER, a single RLK, manages to integrate so many different signals into regulation of cell growth. We set out to determine FER activation by various signals and to identify the cross-talks among these signals. Using FER phosphorylation as a hallmark of its activation, we identified several factors that can activate FER. In particular, its peptide ligand RALF and ABA both activate FER and inhibit root growth, indicating cross-talk between RALF and ABA through FER phosphorylation. We then identified ABA Insensitive 2 (ABI2), a clade A protein phosphatase and a negative regulator of ABA signaling, that directly interacted with and dephosphorylated FER, thus serving as a crucial feedback mechanism for ABA-induced FER activation.

Results and Discussion

FER Phosphorylation Is Induced by RALF or ABA. A hallmark of RLK activation by their ligands is the phosphorylation of the kinase protein, often resulting from self-phosphorylation of the kinase (5). We used phosphorylation status of FER protein as an indicator to monitor the activation of FER in response to various signals. To set up the assay, we raised a polyclonal antibody against FER protein, using the ectodomain (1–446 aa) of FER protein as an antigen. The FER antibody detected a protein band with an apparent molecular mass of about ∼115 kDa in total protein extract from 35-d-old seedlings of Col.0 and C24 WT, but not the two null mutants of FER (*fer-4* and *srn*) (Fig. 1*A* and Fig. S1), suggesting this antibody recognizes the FER protein in the Western blot.

When a protein is phosphorylated, its mass will increase, resulting in mobility-shifted forms in the gel (18). The previous quantitative phosphoproteomics procedure showed that treatment of plants with RALF peptide would trigger the phosphorylation, and thus activation of FER (12). We monitored RALF-induced phosphorylation of FER, using Western blot. We expressed and purified a 6×His·RALF peptide from *Escherichia coli* and confirmed its activity using the RALF-induced root growth inhibition assays. From the results in Fig. S2 *A* and *B*, we concluded that, consistent with the previous work (12), purified RALF peptide inhibited root growth of WT, but not its receptor mutant *fer-4*, confirming RALF activity in our hands. Then we tested whether RALF treatment caused change in the phosphorylation level of FER, using Western blot analysis. We treated the WT plants with 1 μM RALF for 30 min and found that this treatment led to an up-shifted band of FER (from ∼115 to ∼125 kDa), possibly indicating changes in FER phosphorylation status (Fig. 1*B*). We tested whether the up-shifted band (∼125 kDa) represented phosphorylated FER by treatment with a generic phosphatase CIP [alkaline phosphatase from calf intestine, New England Biolabs (NEB)] and the CIP inhibitor (phosphatase inhibitor). We first treated the 3-wk-old WT plants with RALF and then extracted total proteins from treated plants. The protein extract was divided into several aliquots and incubated for 45 min with CIP, CIP plus its inhibitor, and control (without CIP or its inhibitor), respectively. In control or CIP plus its inhibitor, the Western blot showed both the 115- and 125-kDa bands. However, when only CIP was added, the FER protein was detected mainly as a lower band at ∼115 kDa, indicating that the upper band (∼125 kDa) is the phosphorylated FER (we named this band "p-FER"), and the lower mass band

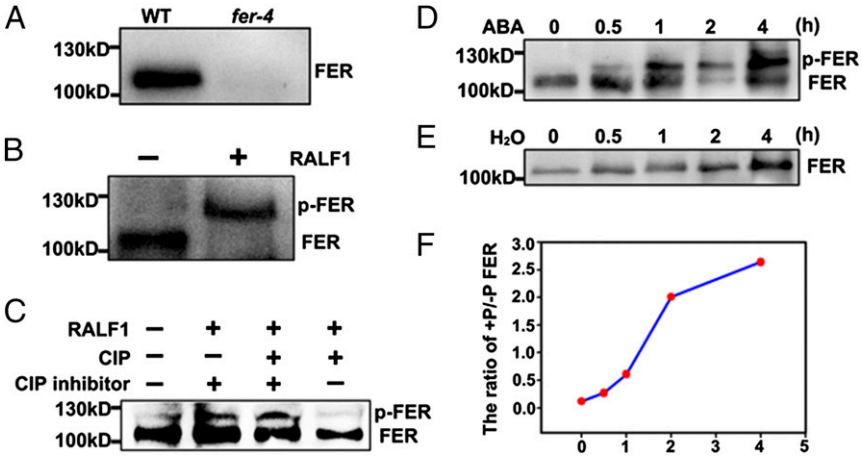

Fig. 1. RALF peptide and ABA enhance FER phosphorylation. (*A*) Specificity analysis of FER antibody. Total protein was extracted from leaves of 35-d-old WT and *fer-4* mutant plants and was analyzed using the FER antibody in a Western blot procedure. (*B*) RALF peptide increased the level of phosphorylated FER protein in plants. Leaves of 3-wk-old WT plants were sprayed with buffer or buffer containing 1 μM RALF peptide, and total proteins were extracted 30 min after the spray for immunoblotting analysis, using the FER antibody. Three separate experiments were conducted and similar results were observed. (*C*) CIP dephosphorylated FER. Total protein was extracted from 3-wk-old WT plants and incubated with (+) or without (–) CIP for 45 min before Western blot analysis. Two separate experiments were conducted, and similar results were obtained. (*D*) FER phosphorylation activated by ABA treatments. Thirty-five-day-old plants were sprayed with 10 μM ABA, and leaves were harvested and total protein was analyzed by immunoblotting using FER antibody. Five independent experiments were conducted showing the same results and a representative blot is shown. (*E*) FER phosphorylation level after H_2O treatment (as a control for *D*). (*F*) Ratios of phosphorylated FER (p-FER)/dephosphorylated FER (FER) that are shown in Fig. 1*D*.

(~115 kDa) of FER is dephosphorylated FER (we named this band "FER") (Fig. 1*C*). Next, we used the same assay to monitor FER activation on ABA treatments. We treated 35-d-old WT plants by spraying 10 μM ABA on the leaves and then collected the leaves at the indicated points. Total protein was extracted, and the p-FER/FER ratio was analyzed using Western blot. We found that FER phosphorylation level, as indicated by p-FER/FER ratio, increased from 0.12 to 2.64 after treatment for 4 h (Fig. 1 *D* and *F*). In parallel, the control treatment using H_2O did not change this ratio (Fig. 1*E*). This result indicated that ABA, similar to RALF, also activated FER. It is of particular interest to note that FER has been previously shown to negatively regulate ABA response through activation of ABI2 via a GEF-ROP/ARAC pathway (17). Taken together, these data suggest that signaling pathways for RALF and ABA closely interact with each other.

***FER* Controls Several Abiotic Stress Responses in Plants.** Because ABA is considered a stress hormone, and previous studies have shown that ABA response mutants often show altered stress sensitivity (19, 20), we reasoned that *fer* mutants may have altered stress responses. To test this hypothesis, we performed stress assay on the WT and *fer* mutant plants. When germinated in normal 1/2 Murashige and Skoog (MS) and then transferred to 1/2 MS medium containing 100 mM NaCl, root growth in *fer-4* mutant is more severely inhibited compared with WT (0.59 ± 0.07 cm in mutant vs. 1.52 ± 0.13 cm in WT; $P < 0.001$), and *fer-4* seedlings died more rapidly on the high-salt medium (Fig. 2 *A* and *C*). This NaCl-sensitive phenotype may have been caused by ionic toxicity or osmotic stress (21). We then treated seedlings with 1/2 MS medium containing 300 mM mannitol (as a hyperosmotic condition) and found that *fer-4* seedlings were less sensitive to the mannitol stress compared with WT (Fig. 2 *A* and *C*). We concluded that *fer-4* was more sensitive to ionic toxicity, but less sensitive to osmotic stress in root growth.

Apart from salt and osmotic stress, extreme growth temperatures, either high or low, are also major forms of abiotic stress for plants. To test whether FER plays a role in temperature stress, we first treated seedlings with heat stress. Both WT and mutant seedlings were incubated at 37 °C for 1.5 h, then transferred to 45 °C for 2.5 h, followed by incubation at normal condition (22 °C) for 4 d. We found that compared with WT, *fer-4* seedlings were more sensitive to heat treatments, as indicated by seedling survival rate [27 ± 1.8% in mutant vs. 70 ± 6.45% in WT ($P < 0.001$); the bleached seedlings were considered dead]. In the cold treatment, 5-d seedlings were treated at −20 °C for 1 h, then transferred to 4 °C for 6 h, followed by growth under normal condition for 3 d. The results indicated that *fer-4* was hypersensitive to cold stress, as indicated by a lower survival rate (16 ± 1.9% in mutant vs. 90 ± 0.96% in WT; $P < 0.001$) (Fig. 2 *B* and *C*).

ABA- and Stress-Hypersensitive Responses in *fer* Mutant Can Be Partially Rescued by the *abi2-1* Gain-of-Function Mutation. As we previously reported (17), FER-GEF1/4/10-ROP11 pathway negatively regulates ABA response by activation of ABI2, a negative regulator of ABA signaling. It is possible that lack of both activation of ABI2 and inhibition of ABA response may also be responsible for changes in stress sensitivity in the *fer* mutants. We tested this idea by genetic analysis of *abi2-1*/*fer* double mutants. Importantly, we used *abi2-1*, a gain-of-function mutant of ABI2 in which ABI2 phosphatase activity is insensitive to inhibition by ABA (3). Thus, in *fer* loss-of-function mutant, an *abi2-1* allele should compensate lack of FER function regarding ABI2 activation (3). We first crossed the *abi2-1* mutant with the *fer* mutant and obtained a homozygous *abi2-1*/*fer* double mutant among the F2 plants (in Ler background). We analyzed the double mutant, single mutants, and the WT in ABA responses and found that *abi2-1* mutation indeed partially rescued the ABA hypersensitive phenotype of *fer* single mutant. In the stomatal response assay, *abi2-1*/*fer* double mutant was less sensitive to ABA than the single *fer* mutant in their stomatal aperture (2.33 ± 0.18 μm in double mutant vs. 1.14 ± 0.12 μm in the single *fer* mutant; $P < 0.001$), but

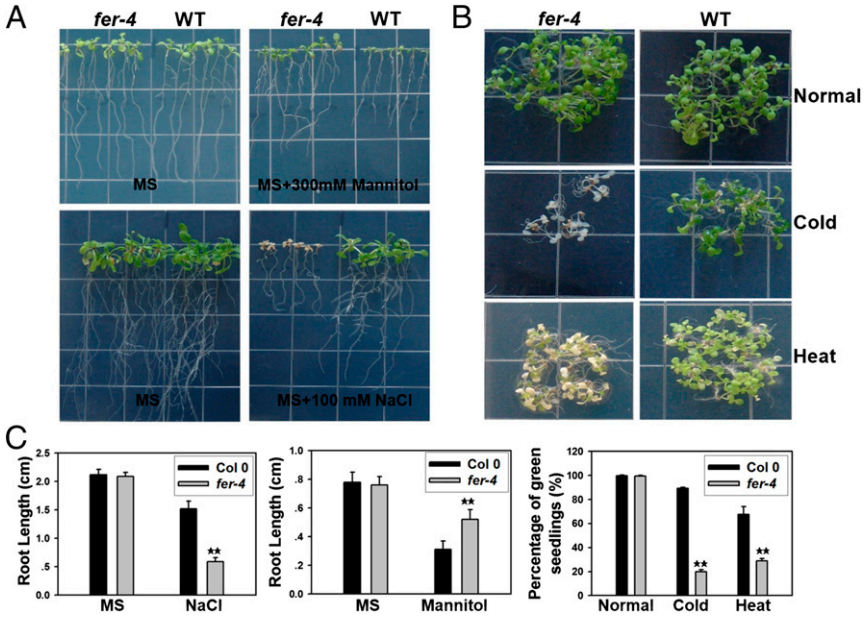

Fig. 2. Altered stress tolerance in *fer* mutant plants. (*A*) The *fer* mutant plants were more sensitive to salt, but less sensitive to mannitol treatments. Four-day-old seedlings were transferred to the 1/2 MS medium supplemented with NaCl or mannitol and grown for 11 d on salt and 4 d on mannitol before taking the photographs. Five independent experiments were conducted for each treatment, showing the same results, and a representative picture is shown. (*B*) The *fer* mutant was more sensitive to cold and heat treatments. Five-day-old seedlings on 1/2 MS medium were treated with cold and heat stress, as described in *Materials and Methods*. Four independent experiments were conducted, showing similar results, and a representative picture was shown for each treatment. (*C*) Root length of the WT and *fer* mutant under NaCl or mannitol treatment in *A*, and seedling survival rate (% green seedlings) under heat or cold treatment in *B*. Data represent average ± SD, and four separate experiments were conducted showing a similar result.

the double mutant is still more sensitive than WT in ABA response (2.33 ± 0.18 μm vs. 2.84 ± 0.16 μm; $P < 0.01$) (Fig. 3*A*). We further performed root growth assay in response to ABA inhibition and found that *abi2-1*/*fer* was also less sensitive to ABA than *fer*, as indicated by primary root length (0.79 ± 0.07 cm vs. 0.54 ± 0.06 cm; $P < 0.001$) (Fig. 3*B*).

We examined whether FER-mediated regulation of ABA pathway controls the ABA-responsive gene expression. We treated Ler, *fer*, *abi2-1*, and *abi2-1*/*fer* with ABA and analyzed the transcript level of four ABA response marker genes (*RD29B*, *ABI5*, *KIN1*, and *RAB18*) in mutants and WT (*Ler*) plants. The data suggest that all four ABA-regulated genes were expressed at a higher level in the *fer* single mutant compared with the double mutant, indicating that constitutively active form of ABI2 in the *abi2-1* mutant compensated loss of function of FER in the *fer* mutant in ABA response (Fig. 3*C*).

As ABA plays a key role in the stress response, we speculated that the stress response defect in *fer* mutant may also be suppressed by the *abi2-1* mutation. We used the *abi2-1*/*fer* double mutant in stress assays to compare with the *fer* single mutant and found that *abi2-1* mutation indeed reduced salt sensitivity in the *fer* mutant, as shown by primary root length (0.96 ± 0.06 cm vs. 0.48 ± 0.09 cm; $P < 0.001$) (Fig. 3*B*). However, responses to cold, heat, and mannitol stress were not altered by *abi2-1* mutation. These data indicated that FER may control the salt stress response through ABI2-mediated ABA signaling pathway.

FER Interacted with the ABA Coreceptors, ABI2, at the Plasma Membrane. To identify the proteins that regulate FER kinase activity through ABA signaling pathway, we screened a yeast two-hybrid (Y2H) cDNA library, using FER kinase domain as a "bait," and identified several interacting proteins. These included ABI2 phosphatase domain that is clearly functionally relevant concerning ABA response (3). Our previous work has shown that FER-GEF1/4/10-ROP11 pathway can activate ABI2 phosphatase activity through physical interaction between ROP11 with ABI2 (17). It is intriguing that ABI2 can also directly interact with FER. Because ABA treatments activated FER, as reflected by increased FER phosphorylation, it is tempting to speculate that ABA activation of FER could be functionally linked through ABI2 interaction with FER. We decided to further examine the FER-ABI2 interaction. We first confirmed that the full length of ABI2, similar to the phosphatase domain, can also interact with FER kinase domain in the Y2H assay (Fig. 4 *A* and *B*). Then we tested several truncated versions of ABI2 and FER protein to identify the domains responsible for the interaction. The results suggest that the C-terminal catalytic/phosphatase domain (150–423 aa,

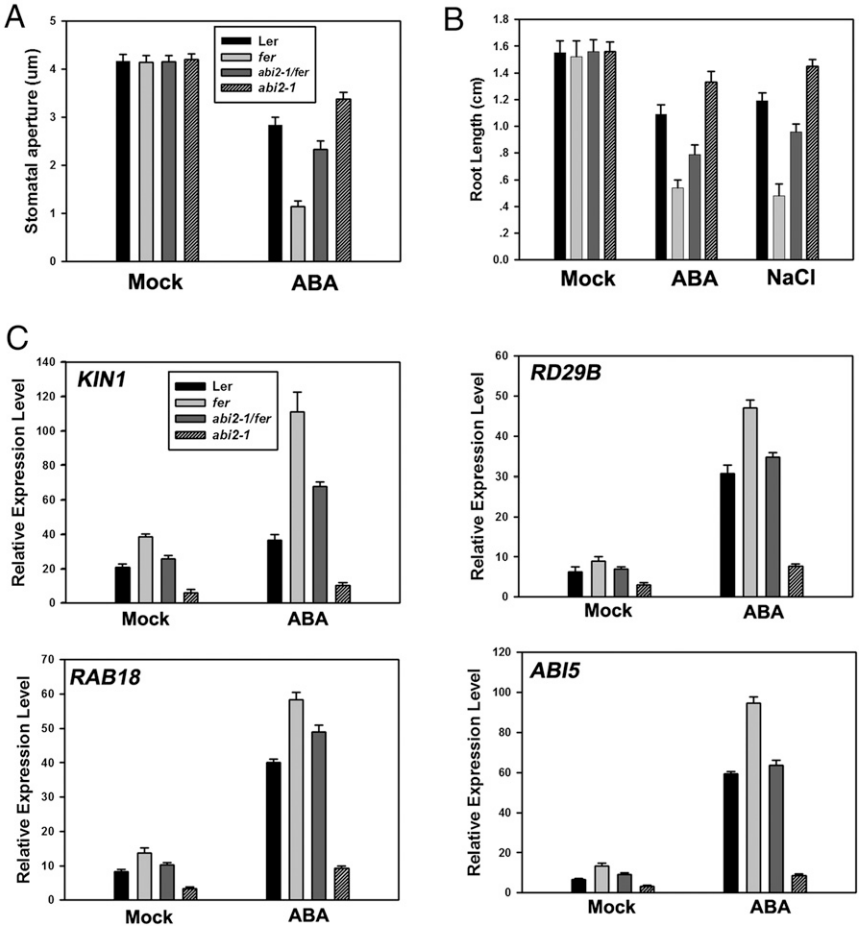

Fig. 3. The *abi2-1* gain-of-function mutation reduced ABA and salt sensitivity of *fer* mutant. (*A*) Measurement of stomatal aperture in *fer single* and *abi2-1*/*fer* double mutant in response to ABA. Data are presented as average value ± SE of three replicates with 16 apertures each. (*B*) Sensitivity to ABA- or NaCl-induced growth inhibition. Five-day-old seedlings (grown on 1/2 MS medium) were transferred to 1/2 MS containing 10 μM ABA, and root length was measured after 6 d. Data represent average ± SE of two independent experiments ($n = 17$ roots per sample). In salt treatment, 5-d-old seedlings (grown on 1/2 MS) were transferred to 1/2 MS containing 100 mM NaCl, and root length was measured after 6 d of growth. Data represent average ± SE of two independent experiments ($n = 17$ roots per sample). (*C*) Expression levels of ABA response genes. Seven-day-old seedlings grown on 1/2 MS were treated with 10 μM ABA, and mRNA levels were analyzed using quantitative RT-PCR. Data represent average ± SD, and three separate experiments were conducted showing a similar result.

ABI2-C), but not the N-terminal noncatalytic domain (1–150 aa, ABI2-N), of ABI2 interacted with the kinase domain of FER (469–896 aa, FER-K). When the FER kinase domain was divided into two shorter domains (469–629 aa, FER-KN; and 629–896 aa, FER-KC), neither of them interacted with ABI2 (Fig. 4*B*).

Studies have shown that clade A PP2C subfamily members function redundantly (1–3), so we tested the interaction between FER and different members in the clade A PP2C subfamily and kinase-associated protein phosphatase (KAPP), a PP2C unrelated to clade A PP2Cs, using Y2H assays. The results showed that the interaction between FER and PP2C A-type phosphatases was selective to some extent. Among the nine clade A PP2Cs, HAB1, HAB2, ABI1, and ABI2 interacted with FER, but the other 5 members and KAPP did not (Fig. S3). This is consistent with the genetic analyses showing important function of ABI1, ABI2, HAB1, and HAB2 in ABA responses (1–3).

Next, we further examined interactions between ABI2 and FER, using several other procedures. First, we tested this interaction, using GST pull-down assay. We purified FER kinase domain (FER-KD) fused with His tag and ABI2 protein fused with GST tag (Fig. S4). We loaded His-tagged FER-KD to the glutathione beads bound with GST-ABI2 and found that ABI2 can pull down FER-KD specifically (Fig. 4*C*). Interestingly, we found that ATP enhanced the interaction between ABI2 and FER during the pull-down assay, but the kinase-dead form of FER (K565R) mutation (9) showed less interaction, suggesting FER kinase activity may be important for the FER-ABI2 interaction (Fig. S5 *A* and *B*). This is also consistent with the result that only the full length of FER kinase domain interacted with ABI2, but each of the two halves did not (Fig. 4*B*). We then used the GST-ABI2 fusion protein to pull down FER protein from total protein extracted from *Arabidopsis* seedlings and again found that FER was copurified with GST-ABI2 fusion on the glutathione beads (Fig. 4*D*). We further performed bimolecular fluorescence complementation (BiFC) assays to test the interaction between ABI2 and FER. When ABI2 tagged with C-terminal CFP (cCFP) and FER tagged with N-terminal Venus (nVenus) were coexpressed in *Arabidopsis* mesophyll protoplasts, fluorescence was detected at the plasma membrane (Fig. 4*E*), but a negative control (cCFP and FER-nVenus) did not yield detectable fluorescence signal (Fig. 4*E*). Finally, we tested the interaction between FER and ABI2, using coimmunoprecipitation (Co-IP). We produced a polyclonal antibody against full-length ABI2 protein and showed that this antibody recognized ABI2, but not other PP2CA members (Fig. S6*A*). The Co-IP assay indicated that FER was associated with ABI2 *in vivo* (Fig. 4*F*). To check whether FER also interacted with other ABI2-type phosphatases, we detected the interaction between FER-FLAG and ABI1, using Co-IP assay (Fig. S6*B*). Consistent with the later genetic assay, FER appears to functionally interact with several closely related PP2C-A members.

ABI2 Inhibits FER Phosphorylation. Earlier studies have shown that RLKs are activated by autophosphorylation and inactivated by dephosphorylation by protein phosphatases, including KAPP-type PP2Cs (22–24). Although ABI2 is in a different subfamily from KAPP, its physical interaction with FER indicates ABI2 may dephosphorylate FER. We decided to monitor the phosphorylation status of FER protein from plant extract to examine the effect of ABI2. When we added purified ABI2-GST to the protein extract from 7-d-old WT plant, we found that ABI2 reduced the amount of p-FER and p-FER/FER ratio 5 min after the addition, indicating that ABI2 dephosphorylated FER (Fig. 5*A*).

To further confirm that this dephosphorylation happened in vivo and is functionally relevant, we examined FER phosphorylation status in gain-of-function *abi2-1* mutants. Using the WT (Ler background) as control, we found that p-FER/FER level was significantly reduced in the *abi2-1* mutant with or without ABA treatment (Fig. 5*B*). Those results indicated that high ABI phosphatase activity in *abi2-1* mutant reduced the p-FER level in

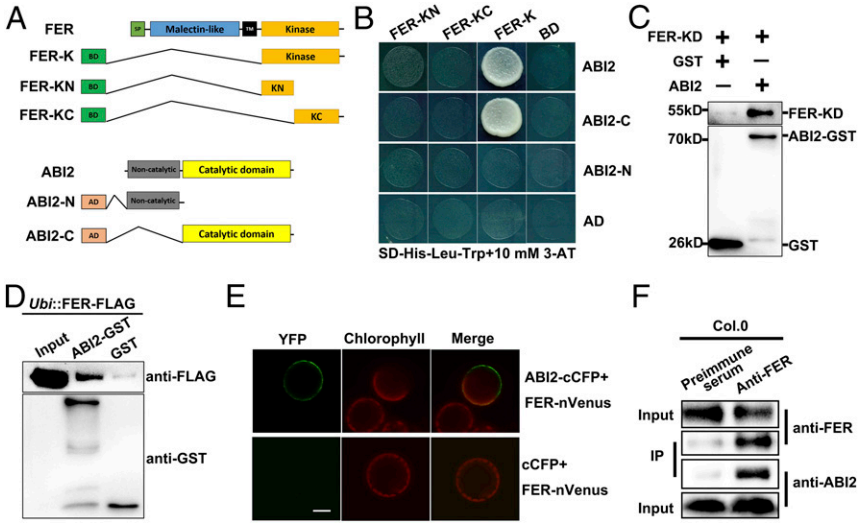

Fig. 4. Interaction between FER and ABI2. (*A*) Diagram of the full-length and truncated FER and ABI2 constructs with specific deletions. The FER protein contains a signal peptide domain (SP), a malectin-like extracellular domain (malectin-like), a transmembrane domain (TM), and a cytosolic kinase domain. ABI2 contains a catalytic domain at the C-terminal region and a noncatalytic domain at the *N*-terminal region. (*B*) Interaction between FER and ABI2 in the yeast two-hybrid system. BD, binding domain vector (pGBKT7); AD, activation domain vector (pGADT7); 3-AT, 3-amino-1, 2, 4-triazole. Yeast cells harboring different constructs were grown on synthetic dropout medium for 4 d before taking the photographs. (*C*) GST pull-down assay using recombinant proteins from *E. coli*. GST (27 kDa) or GST-ABI2 (70 kDa) protein was bound to beads and then incubated with 6×His-tagged FER (55 kDa). The eluted proteins were separated by SDS/PAGE and probed with anti-His (*Upper*) or anti-GST (*Lower*) antibody. Image represents one of triplicated experiments showing the same results. (*D*) GST pull-down assay using plant proteins. Total protein was extracted from 7-d-old *Ubi*::FER-FLAG transgenic seedlings and incubated with glutathione beads (preincubated with GST-ABI2 or GST) for 3 h before Western blot analysis. (*E*) Interaction between FER and ABI2 in the BiFC system. YFP image for the interacting FER-nVenus and ABI2-cCFP was observed with GFP filter. Chlorophyll autofluorescence is shown red. The negative controls expressing FER-nVenus and cCFP failed to yield detectable green fluorescence. Four separate experiments were conducted showing a similar result. (Scale bar, 20 μm.) (*F*) Interaction between ABI2 and FER, as detected by Co-IP assay. Three independent experiments were conducted showing similar results, and one representative blot is shown.

plants, supporting the conclusion that ABI2 dephosphorylates FER in vivo.

ABI2–FER Interaction Mediates RALF and ABA Cross-Talk and Controls the Root Growth in Plants. As ABI2 interacted with and dephosphorylated FER (Fig. 5*A*), and we observed activation of FER by ABA (Fig. 1 *D* and *F*), we reasoned that ABA may activate FER through the PYR/PYL/RCAR (ABA) -ABI2 pathway. To test this possibility, we first used the gel shift assay to monitor FER dephosphorylation by ABI2 in vitro, using the purified ABI2 and FER-kinase protein (Fig. S4). As shown in Fig. 5*C*, both ABI2 and CIP can dephosphorylate FER-kinase protein, and phosphatase inhibitor hampered the effect of the phosphatases (Fig. 5*C*). We then tested the function of PYR/PYL/RCAR (ABA) in this assay by adding either PYL1 alone or together with ABA. We found that adding PYL1 to the ABI2–FER complex did not change the FER phosphorylation level, but when PYL1 and increasing doses of ABA were added together, FER phosphorylation level increased in an ABA dosage-dependent manner (Fig. 5*D* and Fig. S4).

To test whether pFER accumulation in response to ABA is mediated by the PYR/PYL/RCAR (ABA)–PP2Cs core signaling module, we performed genetic analysis of mutants containing mutations in these core components. We first analyzed the pFER level in the *abi1-2*/*abi2-2*/*hab1-1* triple mutant with or without ABA treatment. We found that FER phosphorylation level increased with ABA treatment in the WT plants, but p-FER levels remained high in the *abi1-2*/*abi2-2*/*hab1-1* triple mutant with or without ABA, suggesting these ABI2-type phosphatases inhibit FER activation in plants (Fig. 5*E*). We then examined FER phosphorylation in the ABA receptor mutants, pentuple *pyr1pyl2pyl4pyl5pyl8* (*12458*) and hextuple *pyr1pyl1pyl2pyl4pyl5pyl8* (*112458*) mutants, that were previously shown to be defective in ABA response (25). We treated 35-d-old *12458*, *112458* mutants and WT (Col.0) plants by spraying 10 μM ABA on the leaves for 1 h. Total protein was then extracted and the p-FER/FER ratio analyzed, using Western blot. We found that FER phosphorylation levels again increased upon ABA treatment in the WT plants, but remained low, and ABA did not change the pFER level significantly in *pyr/pyl/rcar* pentuple (*12458*) and hextuple (*112458*) mutants (Fig. 5*F*). To rule out the possibility that PYR/PYL/RCAR family proteins directly interact with FER to regulate its kinase activity, we tested the interaction between FER and some PYR/PYL/RCAR members, using Y2H. Our result showed that FER did not interact directly with PYR/PYL/RCAR (Fig. S7). Taken together, the above results indicated that pFER accumulation in response to ABA is dependent on the PYR/PYL/RCAR-type ABA receptors to inhibit the ABI2/PP2CAs phosphatase activity.

Both RALF and ABA inhibit root growth (Fig. S2 and refs. 4, 12, and 17), and both RALF and ABA activate FER. We suspected that ABA may cross-talk with RALF peptide through the FER–ABI2 interaction to regulate root growth. Because FER activity is reduced in the *abi2-1* mutants (Fig. 5*B*), we speculated that *abi2-1* mutation may alter RALF response through inhibition of FER kinase activity. First, we examined FER phosphorylation level in the *abi2-1* mutant in response to RALF. We found that the FER phosphorylation level in the *abi2-1* mutant was lower than the WT control, either with or without RALF treatment (Fig. 5*G*), indicating that enhanced ABI2 activity in the *abi2-1* mutant

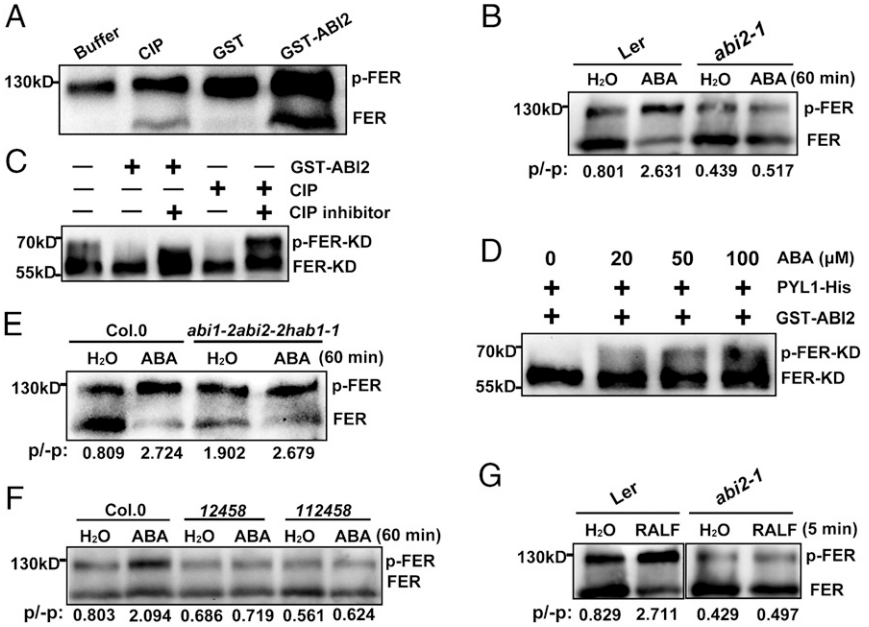

Fig. 5. ABI2 inhibits FER phosphorylation through the PYR/PYL (ABA)-PP2CA pathway. (*A*) ABI2 protein reduced the p-FER level. Total protein extracted from WT leaves was treated with ABI2-GST, GST, and CIP before Western blot analysis. Three independent experiments were conducted showing similar results, and one representative blot is shown. (*B*) ABI2 inhibits FER phosphorylation. Leaves of 3-wk-old Ler and *abi2-1* plants were sprayed with H_2O or 10 μM ABA and harvested 60 min afterward for Western blot analysis. Three independent experiments were conducted, showing similar results, and one representative blot is shown. (*C*) ABI2 dephosphorylates FER in vitro. Purified FER-KD was activated by added ATP and inhibited by ABI2 or CIP. Image is one representative of triplicated experiments showing similar results. (*D*) PYR/PYL (ABA)-ABI2-FER interactions in *vitro*. The purified FER-KD, ABI2, and PYL1 were mixed, and ABA was added as indicted in the figure. Western blot was performed using His antibody. Image is one representative of triplicated experiments showing similar results. (*E*) pFER is inhibited by the clade A protein phosphatase activity. Total protein was extracted from *abi1-2abi2-2hab1-1* mutant and WT (Col.0) leaves (sprayed with H_2O or 10 μM ABA) for Western blot analysis. Three independent experiments were conducted showing similar results, and one representative blot is shown. (*F*) pFER accumulation in response to ABA is PYR/PYL/RCAR-mediated. Four-week-old Col.0, *pyr1pyl2pyl4pyl5pyl8* (*12458*) and *pyr1pyl1pyl2pyl4pyl5pyl8* (*112458*) plants were sprayed with 10 μM ABA before Western blot analysis. Three independent experiments were conducted, showing similar results, and one representative blot is shown. (*G*) ABI2 inhibits FER phosphorylation. Total proteins were extracted from Ler and *abi2-1* leaves (treated 5 min with H_2O or RALF) for Western blot analysis. Three independent experiments were conducted, showing similar results, and one representative blot is shown.

(*abi2-1* protein is refractory to inhibition by endogenous ABA) (26) reduced FER activity in response to RALF response. Then, we treated *abi2-1* and WT plants using RALF peptide to observe their response to RALF in the root inhibition assay. The results showed that *abi2-1* mutants are less sensitive to the RALF peptide in root growth assay compared with WT (Fig. 6*A*; $P < 0.01$). To further test our hypothesis, we performed RALF bioassay using the *abi1-2*/*abi2-2*/*hab1-1*, *pyr1pyl2pyl4pyl5pyl8* (*12458*) and *pyr1pyl1pyl2pyl4pyl5pyl8* (*112458*) mutant seedlings. We found that *abi1-2*/*abi2-2*/*hab1-1* mutant is hypersensitive, but *12458* and *112458* are less sensitive to RALF compared with Col.0 (Fig. 6*B*). This again supported the notion that ABA–RALF signaling cross-talk was mediated by the ABA-receptor-PP2C core signaling modules.

Because both ABA and RALF inhibit root growth, we examined how ABA–RALF interact in this process. We performed dose–response assay of root-growth inhibition by combining RALF and ABA treatments. First, we used variable RALF1 doses in the presence or absence of a fixed level of ABA (5 μM) to observe the effect on root inhibition. We found that presence of ABA enhanced the root growth inhibition by RALF (Fig. 6*C*). Then we changed ABA levels with or without a fixed concentration of RALF (1 μM). Our results showed that presence of RALF reduced the ABA sensitivity in the root growth assay (Fig. 6*D*). These results suggest that ABA enhances RALF action, and RALF suppresses ABA responses in root growth.

***RALF1* Gene Suppression by RNAi Renders ABA Hypersensitivity in the Transgenic Plants.** Our results on ABI2-FER interaction and the finding that *abi2-1* mutant plants are less sensitive to both ABA and RALF peptide strongly suggest that the signaling pathways in response to RALF and ABA interconnect through FER and ABI2 interaction. To further test this idea, we obtained the RALF1-RNAi/*ralf1* plants and examined their response to ABA, using the root growth assay (27). The *ralf1* and WT seeds were first germinated in 1/2 MS and then transferred to 1/2 MS containing various concentrations of ABA. We found that *ralf1* mutants are more sensitive to ABA compared with the WT, showing stronger root growth inhibition by ABA (Fig. 6*E*; $P < 0.01$). This result again supports the conclusion that RALF and ABA, through FER-ABI2 interaction, manifest a signaling cross-talk in the control of plant cell growth.

Concluding Remarks

Plant growth and development are tightly controlled by a battery of hormones working together in a delicate balance. As response pathways to individual hormones are being dissected at the molecular level, the next frontier is to understand the cross-talk mechanisms that govern interactions among plant hormones. We report here a mechanism that mediates interaction of a peptide hormone RALF and a small molecule hormone ABA. As ABA response core regulators, ABI2-type PP2C phosphatases directly interact with and dephosphorylate RALF receptor kinase FER, connecting ABA, which is produced under various stress conditions, with a growth-regulating peptide RALF in root growth control (Fig. 6 *C* and *F*). In a "linear" pathway, ABA binds to its receptors to inhibit PP2C-A, releasing SnRK2 into active forms that can directly inhibit AHA2-mediated acidification and thereby repress root growth (4, 28, 29). The peptide hormone RALF, in contrast, binds and activates receptor FER to directly inhibit AHA2-mediated root growth (12). Further, through a "cross-talk" mode, RALF-FER activates ABI2 through the GEF–ROP pathway (17), leading to a feedback inhibition of ABA response. Thus, when the RALF–FER pathway is disrupted, as in the *fer-4* mutant or *RALF1* knock-down line, ABA response is enhanced. This is consistent with the results showing

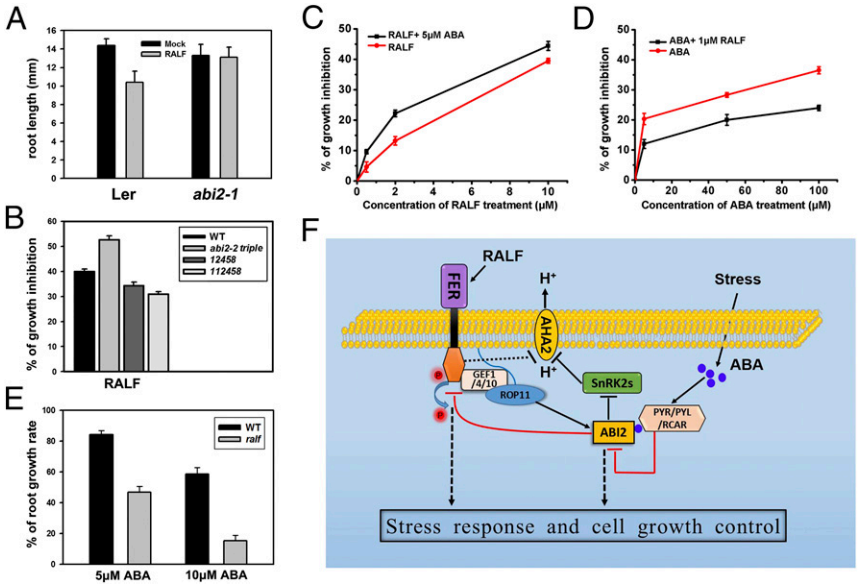

Fig. 6. ABA-RALF signaling cross-talk through ABI2-FER interaction. (A) *abi2-1* mutants were less sensitive to RALF peptide. Root lengths of WT and *abi2-1* were measured ($n = 13$ roots per trial); data represent average ± SD. Four separate experiments were conducted showing a similar result. (*B*) RALF peptide response of *abi1-2abi2-2hab1-1 mutants* (*abi2-2 triple*), *12458*, and *112458* mutants. Root lengths of WT and *abi2-2 triple*, *12458*, and *112458* mutants were measured ($n = 15$ roots per trial); data represent average ± SD. Three separate experiments were conducted showing a similar result. (*C*) Three-day-old Col.0 seedlings were incubated in 1/2 MS liquid medium containing various concentrations of RALF with or without ABA (5 μM). (*D*) Three-day-old Col.0 seedlings were incubated in 1/2 MS liquid medium containing various ABA concentrations with or without RALF (1 μM). (*E*) *RALF1* RNAi (labeled as *ralf1*) seedlings were hypersensitive to ABA in root elongation assay. Seven-day-old *ralf1* and WT seedlings were transferred to 1/2 MS containing ABA and grown for 4 d before root lengths were analyzed. Data represent average ± SE of two independent experiments with 12 seedlings for each data point. (*F*) A working model for ABA-RALF signaling cross-talk through ABI2-FER interaction. ABA directly inhibits AHA2 through activation of SnRK2s. RALF-FER pathway inhibits AHA2 activity to inhibit cell growth, and through activation of the GEF1/4/10-ROP11 pathway, RALF-FER activates ABI2 phosphatase, thereby inhibiting ABA response. Meanwhile, ABI2 interacts with and dephosphorylates FER to inhibit FER-GEF1/4/10-ROP11 pathway. Arrows denote activation, and bars indicate inhibition.

that addition of RALF reduced ABA response in root growth assay (Fig. 6*D*). Addition of ABA, in contrast, enhanced RALF response, consistent with the model that ABA inhibits PP2Cs that suppress FER activity (Fig. 6*F*). Because H^+-ATPases (AHAs) are also regulated by other factors (such as auxin), we expect a number of regulatory pathways may further converge on AHA-based acidification of extracellular space to control plant cell growth.

ABA and RALF also appear to be connected in stress responses. It is well known that ABA functions in plant response to a number of biotic and abiotic stress conditions (1–3). Recent studies also place RALF-FER pathway in pathogen responses (30, 31). Our results here show that FER kinase activity affected by RALF and ABA plays a critical role in abiotic stress responses as the *fer* mutant displayed dramatically altered stress tolerance compared with the WT plants. This could be explained, at least in part, by our finding that FER inhibits ABA response through activation of ABI2 by the GEF1/4/10-ROPP11 network (17). This also further supports the notion that FER acts as a "master" node in the cross-talk of developmental, pathogen, and abiotic stress pathways, as reported earlier (6, 17, 30). However, the full mechanism underlying FER regulation of stress responses may not be entirely dependent on cross-talk with ABA, and other signaling nodes may be involved. Considering the importance of FER in the control of stress response and plant development, identifying other components such as FER coreceptors and downstream molecules will enable us to better understand how plants respond and adapt to environmental cues.

Materials and Methods

FER Antibody and Gel Shift Assays. Partial FER protein (1–446 aa) was fused to GST by cloning into the expression vector pGEX4T-1, using primers FERGST-F and FERGST-R, as shown in Table S1. The construct was transformed into BL21 star (DE3) cells that produced the GST fusion protein under induction by 0.5 mM isopropyl-β-D-thiogalactopyranoside. The GST-fusion protein was purified and used as an antigen to produce a polyclonal antibody in rabbit.

Western blot of FER protein was performed as described previously, with minor modification (18). Protein samples were subjected to electrophoresis on an 8% (wt/vol) SDS/PAGE gel [with 60% (vol/vol) glycerol instead of ddH_2O], using several voltage steps (60 V/1 h, 90 V/1 h, up to 120 V for 5 h). The protein bands were transferred to a nitrocellulose membrane (BioTrace NT; PALL Corporation), using a wet electrophoresis apparatus (100 mA/2 h). The membrane was blocked in 5% (wt/vol) milk/TBST (50 mM Tris·HCl, 150 mM NaCl, 0.1% Tween-20 at pH 7.5) for 1.5 h at room temperature, and then probed with the anti-FER antiserum [1:4,000 dilution in 5% (wt/vol) milk/TBST] at 4 °C overnight. After washing three times (6 min/T) in TBST, the membrane was incubated with goat anti-rabbit IgG [1:6,000 dilution in 5% (wt/vol) milk/TBST; Promega Corporation, W4011] for 1 h, followed by three washes in TBST (6 min/T) and once in TBS. The signal was imaged by ChemiDoc XRS imaging system (Bio-Rad), using the enhanced chemiluminescence method (Thermo Fisher Scientific, 34075).

Protein–Protein Interaction Analysis. FER-kinase domain (469–896 aa, FER-KD) was used as bait in Y2H to screen an *Arabidopsis* seedling cDNA library essentially as described previously (32). Yeast cells AH109 were first transformed with "bait," a plasmid containing FER kinase domain fused to the GAL4 DNA binding domain in the pGBKT7 vector. The yeast cells containing the "bait" were further transformed with the *Arabidopsis* cDNA library cloned in the prey vector pACT, as previously described (32). The transformed cells were plated on synthetic dropout selection medium that lacked Trp, Leu, and His, supplemented with 20 mM 3-AT to reduce the growth of false-positive colonies.

The full-length ABI2 coding sequence was subcloned into the pGADT7 vector, using the primers shown in Table S1, and then cotransformed with FER-KD into yeast strain AH109 to test interaction, as described earlier.

The coding region of *FER* cDNA was amplified by PCR with primers FERBIFCF and FERBIFCR (Table S1) and cloned into plasmid pE3308. Coding sequence of *ABI2* was prepared in the same way and cloned into the plasmid pE3449. We performed BiFC assays in vivo as, described earlier (33). Briefly, protoplasts were isolated from 3-wk-old *Arabidopsis* rosette leaves, as described previously (33). All the chemicals used in protoplast isolation were obtained from Sigma. Leaf strips were incubated in enzyme solution (0.4 M mannitol, 20 mM KCl, 1.5% cellulase R10, 0.4% macerozyme R10, 10 mM $CaCl_2$, 0.1% BSA, 20 mM Mes at pH 5.7) in the dark for 3 h at room temperature under gentle rotation (30–40 rpm). During the last 1–2 min of incubation, the speed of rotation was increased to ∼100 rpm. Protoplasts were washed two times with W5 solution (154 mM NaCl, 125 mM $CaCl_2$, 5 mM KCl, 2 mM Mes at pH 5.7) and centrifuged at 100 × *g* for 5 min, and protoplasts were resuspended in MMg (0.6 M mannitol, 15 mM $MgCl_2$, 4 mM Mes at pH 5.7) solution. For transfection, 100 μL protoplasts were mixed thoroughly with 40 μg plasmid DNA and 110 μL 40% (wt/vol) PEG [0.6 M mannitol, 100 mM $CaCl_2$, 40% (wt/vol) PEG3350]. The mixture was incubated for 10 min at room temperature under dark and before adding 440 μL W5 solution. The protoplasts were collected by centrifugation at 100 × *g* for 2 min and washed twice with W5 solution. After the second wash, cells were resuspend in 1 mL W5 and incubated at 23 °C under dark for 16 h. For fluorescence detection, cells were examined under a confocal microscope with excitation light at 488 nm.

For the pull-down assays, FER kinase domain was subcloned into pET28a using primers FER-kinase-F and FER-kinase-R (Table S1) to produce an 6xHis-FER-KD fusion protein, and expressed in *E. coli* (BL21:DE3). After overnight induction at 16 °C with 0.5 mM IPTG, the bacteria were pelleted by centrifugation, resuspended in 100 mL lysis buffer (20 mM Tris·HCl, 150 mM NaCl, 10 mM imidazole, 1 mM PMSF and 0.5% Triton X-100 at pH 7.4), and sonicated. The soluble 6xHis-FER-KD fusion protein was affinity-purified using a HisTrap FF column (GE Healthcare) according to the manufacturer's instructions. Two micrograms GST or GST-ABI2 were incubated with 2 μg His-FER-KD in 300 μL binding buffer [20 mM Hepes, 40 mM KCl, 1 mM EDTA, 0.05% Triton X-100, 1 mM DTT, and 1 mM protease inhibitor mixture (cOmplete EDTA-free; Roche #04693132001) at pH 7.5] under agitation at 4 °C. Glutathione–agarose beads (30 μL) were added after 3 h incubation and mixed for another 3 h at 4 °C. Beads were collected by centrifugation and washed five times with wash buffer (20 mM Tris·HCl, 150 mM NaCl, 1 mM EDTA, and 0.05% Triton X-100 at pH 7.4). The proteins on the beads were resolved by 10% (wt/vol) SDS/PAGE and detected by immunoblotting using a GST or His antibody.

For pull-down assay using plant extract, *Ubi*::FER-FLAG transgenic seedlings were ground in liquid nitrogen, and tissue powder was resuspended in extraction buffer (50 mM Tris·HCl at pH 7.5, 150 mM NaCl, 1 mM EDTA, 5% (vol/vol) glycerol, and protease inhibitor) containing 1% Triton X-100. The suspensions were centrifuged at 20,000 × *g* for 15 min, and the resulting supernatant was incubated with glutathione beads that were preincubated with GST-ABI2 or GST. After 3 h incubation, beads were washed three times with the extraction buffer containing 0.1% Triton X-100 and boiled in 1 × SDS/PAGE loading buffer and analyzed by SDS/PAGE and immunoblotting.

For Co-IP assay, 7-d-old Col.0 seedlings and FER-FLAG transgenic seedlings were ground in liquid nitrogen, and tissue powder was resuspended in Co-IP buffer (50 mM Tris·HCl at pH 7.5, 150 mM NaCl, 1 mM EDTA, 5% (vol/vol) glycerol, and protease inhibitor mixture) containing 1% Triton X-100 and 50 μM MG132. Homogenate was centrifugation at 20,000 × *g* for 15 min. Then supernatant was incubated with A/G agarose preincubated with anti-FER for interaction between FER and ABI2, or with M2 agarose gel for interaction between FER-FLAG and ABI1. The incubation continued for 4 h at 4 °C, and then the agarose beads were washed five times with the extraction buffer containing 0.1% triton X-100. The immunoprecipitates associated with the agarose gel were boiled in SDS/PAGE loading buffer, analyzed by SDS/PAGE, and transferred to nitrocellulose membrane for detection with anti-FER, anti-FLAG, anti-ABI2, or anti-ABI1 (34) antibody.

Gene Expression Studies. For the analysis of ABA-induced gene expression, WT (Ler), *fer*, *fer/abi2-1* seedlings were treated with ABA as described (17). Total RNA was prepared with TRIzol (Invitrogen) from mixed tissues of *Arabidopsis*. Two micrograms total RNA were reverse-transcribed to cDNA, using a kit from Invitrogen, after DNase treatment. The cDNA products were diluted 20-fold to be used as template in PCR analysis. The transcripts of ABA response marker genes were measured by quantitative RT-PCR, using SYBR premix ExTaqTM (Takara) with a CFX96 Touch Real-Time PCR Detection System (Bio-Rad Pacific Ltd). Each sample was measured three times, and a representative value was presented in the figure.

FER Dephosphorylation Assays. Three-week-old *Arabidopsis* rosette leaves were homogenized in 80 μL calf intestinal alkaline phosphatase buffer (100 mM NaCl, 50 mM Tris·HCl at pH 7.9, 10 mM $MgCl_2$, and 1 mM DTT) containing 0.5% Triton X-100 and divided into two aliquots and preheated at 65 °C for 10 min to inactivate endogenous enzymes. Alkaline phosphatase (New England Biolabs) or ABI2-GST was added to one of the two aliquots, and both were incubated at 30 °C for 5 min. The dephosphorylation reactions were stopped by adding 10 μL 5 × SDS/PAGE sample buffer and boiling for 10 min. The samples were examined by immunoblot analysis as described earlier.

For the PYL1(ABA)-ABI2-FER reconstitution assays, His-FER-KD (2.5 μg), His-PYL1 (3 μg), GST-ABI2 (4 μg), and ABA (0, 20 μM, 50 μM, or 100 μM) were

added in 50 μL of kinase buffer (25 mM Tris·HCl at pH 7.5, 10 mM $MgCl_2$, 1 mM $CaCl_2$, 1 mM DTT, and 2 mM ATP) and incubated at 30 °C for 1 h. The reactions were terminated by adding 15 μL of 4×SDS/PAGE loading buffer and resolved by 10% (wt/vol) SDS/PAGE, His-FER-KD was detected by immunoblotting, using anti-His polyclonal antibody (Abmart Corporation).

Plant Materials and Phenotype Analysis. Plants were grown at 22 °C under 16-h-light/8-h-dark cycles. Seeds for the mutant lines were purchased from the ABRC (*Arabidopsis* Biological Resource Center) and GABI-Kat collections. The *abi2-1/fer* double mutant was produced by crossing *abi2-1* (ABRC# CS23) and *fer* mutant (9). *pyr1pyl2pyl4pyl5pyl8* (*12458*), *pyr1pyl1pyl2pyl4pyl5pyl8* (*112458*), *hab1-1abi1-2abi2-2* mutant lines were isolated as described previously (25, 35).

For stomatal assays, WT (Ler), *fer*, *abi2-1/fer* plant leaves were floated on stomatal opening buffer (5 mM Mes, 5 mM KCl, 50 μM $CaCl_2$, pH 5.6) under light for 6 h and then treated with 1 μM ABA (Sangon Biotech) for 1 h. Thereafter, stomatal apertures were measured as described (17).

For the stress treatment, *Arabidopsis* seeds were surface-sterilized and germinated on 1/2 MS medium supplemented with 1% sucrose and solidified by 0.9% agar. ABA, NaCl, or mannitol was included into the medium at concentrations indicated in the figures. For heat treatment, 5-d seedlings were treated at 37 °C for 1.5 h, 45 °C for 2.5 h, and then transferred to 22 °C for four days. For cold treatment, five-day seedlings were treated at −20 °C for 1 h, 4 °C for 6 h, and then grown under 22 °C for three days.

For RALF peptide response assay, seeds were surface-sterilized and stratified at 4 °C for 2 d. The seeds were then transferred to 1/2 strength MS agar medium and grown for 5 d at 22 °C under 16-h-light/8-h-dark cycles. The 5-d-old seedlings were transferred to the liquid 1/2 MS medium containing 1 μM RALF peptide (27) and grown for 3 more days, followed by photographing and measurement of root length.

ACKNOWLEDGMENTS. We thank Dr. Alice Cheung, Dr. Daniel Moura, Grossniklaus Ueli, Dr. Jigang Li, and Dr. Nieng Yan for providing plant, ABI1 antibody, or plasmid materials, and Dr. Legong Li for assistance in laser confocal microscopy. This work was supported by grants from National Natural Science Foundation of China (NSFC-31400232, 31571444), the State Key Laboratory of Molecular Developmental Biology (2015-MDB-KF-12), the Fundamental Research Funds for the Central Universities of China, and a grant from the National Science Foundation.

1. Raghavendra AS, Gonugunta VK, Christmann A, Grill E (2010) ABA perception and signalling. *Trends Plant Sci* 15(7):395–401.
2. Cutler SR, Rodriguez PL, Finkelstein RR, Abrams SR (2010) Abscisic acid: Emergence of a core signaling network. *Annu Rev Plant Biol* 61:651–679.
3. Hubbard KE, Nishimura N, Hitomi K, Getzoff ED, Schroeder JI (2010) Early abscisic acid signal transduction mechanisms: Newly discovered components and newly emerging questions. *Genes Dev* 24(16):1695–1708.
4. Planes MD, et al. (2015) A mechanism of growth inhibition by abscisic acid in germinating seeds of *Arabidopsis thaliana* based on inhibition of plasma membrane H^+-ATPase and decreased cytosolic pH, K^+, and anions. *J Exp Bot* 66(3):813–825.
5. Shiu SH, Bleecker AB (2001) Receptor-like kinases from *Arabidopsis* form a monophyletic gene family related to animal receptor kinases. *Proc Natl Acad Sci USA* 98(19): 10763–10768.
6. Nibau C, Cheung AY (2011) New insights into the functional roles of *Cr*RLKs in the control of plant cell growth and development. *Plant Signal Behav* 6(5):655–659.
7. Wolf S, Hématy K, Höfte H (2012) Growth control and cell wall signaling in plants. *Annu Rev Plant Biol* 63:381–407.
8. Hématy K, et al. (2007) A receptor-like kinase mediates the response of Arabidopsis cells to the inhibition of cellulose synthesis. *Curr Biol* 17(11):922–931.
9. Escobar-Restrepo JM, et al. (2007) The FERONIA receptor-like kinase mediates male-female interactions during pollen tube reception. *Science* 317(5838):656–660.
10. Duan Q, et al. (2014) Reactive oxygen species mediate pollen tube rupture to release sperm for fertilization in *Arabidopsis*. *Nat Commun* 5:3129.
11. Ngo QA, Vogler H, Lituiev DS, Nestorova A, Grossniklaus U (2014) A calcium dialog mediated by the FERONIA signal transduction pathway controls plant sperm delivery. *Dev Cell* 29(4):491–500.
12. Haruta M, Sabat G, Stecker K, Minkoff BB, Sussman MR (2014) A peptide hormone and its receptor protein kinase regulate plant cell expansion. *Science* 343(6169): 408–411.
13. Yu F, et al. (2014) FERONIA receptor kinase controls seed size in *Arabidopsis* thaliana. *Mol Plant* 7(5):920–922.
14. Duan Q, Kita D, Li C, Cheung AY, Wu HM (2010) FERONIA receptor-like kinase regulates RHO GTPase signaling of root hair development. *Proc Natl Acad Sci USA* 107(41): 17821–17826.
15. Guo H, et al. (2009) Three related receptor-like kinases are required for optimal cell elongation in *Arabidopsis thaliana*. *Proc Natl Acad Sci USA* 106(18):7648–7653.
16. Deslauriers SD, Larsen PB (2010) FERONIA is a key modulator of brassinosteroid and ethylene responsiveness in *Arabidopsis* hypocotyls. *Mol Plant* 3(3):626–640.
17. Yu F, et al. (2012) FERONIA receptor kinase pathway suppresses abscisic acid signaling in *Arabidopsis* by activating ABI2 phosphatase. *Proc Natl Acad Sci USA* 109(36): 14693–14698.
18. Yu X, et al. (2007) *Arabidopsis* cryptochrome 2 completes its posttranslational life cycle in the nucleus. *Plant Cell* 19(10):3146–3156.
19. Pandey GK, et al. (2004) The calcium sensor calcineurin B-like 9 modulates abscisic acid sensitivity and biosynthesis in *Arabidopsis*. *Plant Cell* 16(7):1912–1924.
20. Smalle J, et al. (2003) The pleiotropic role of the 26S proteasome subunit RPN10 in *Arabidopsis* growth and development supports a substrate-specific function in abscisic acid signaling. *Plant Cell* 15(4):965–980.
21. Munns R, Schachtman DP, Condon AG (1995) The significance of a two-phase growth response to salinity in wheat and barley. *Aust J Plant Physiol* 22(4):561–569.
22. Li J, Smith GP, Walker JC (1999) Kinase interaction domain of kinase-associated protein phosphatase, a phosphoprotein-binding domain. *Proc Natl Acad Sci USA* 96(14):7821–7826.
23. Shah K, Russinova E, Gadella TW, Jr, Willemse J, De Vries SC (2002) The *Arabidopsis* kinase-associated protein phosphatase controls internalization of the somatic embryogenesis receptor kinase 1. *Genes Dev* 16(13):1707–1720.
24. Hua D, et al. (2012) A plasma membrane receptor kinase, GHR1, mediates abscisic acid- and hydrogen peroxide-regulated stomatal movement in *Arabidopsis*. *Plant Cell* 24(6):2546–2561.
25. Gonzalez-Guzman M, et al. (2012) Arabidopsis PYR/PYL/RCAR receptors play a major role in quantitative regulation of stomatal aperture and transcriptional response to abscisic acid. *Plant Cell* 24(6):2483–2496.
26. Santiago J, et al. (2012) Structural insights into PYR/PYL/RCAR ABA receptors and PP2Cs. *Plant Sci* 182:3–11.
27. Bergonci T, et al. (2014) *Arabidopsis thaliana* RALF1 opposes brassinosteroid effects on root cell elongation and lateral root formation. *J Exp Bot* 65(8):2219–2230.
28. Merlot S, et al. (2007) Constitutive activation of a plasma membrane H(+)-ATPase prevents abscisic acid-mediated stomatal closure. *EMBO J* 26(13):3216–3226.
29. Hayashi Y, Takahashi K, Inoue S, Kinoshita T (2014) Abscisic acid suppresses hypocotyl elongation by dephosphorylating plasma membrane H(+)-ATPase in *Arabidopsis thaliana*. *Plant Cell Physiol* 55(4):845–853.
30. Cheung AY, Wu HM (2011) THESEUS 1, FERONIA and relatives: A family of cell wall-sensing receptor kinases? *Curr Opin Plant Biol* 14(6):632–641.
31. Boisson-Dernier A, Kessler SA, Grossniklaus U (2011) The walls have ears: The role of plant *Cr*RLK1Ls in sensing and transducing extracellular signals. *J Exp Bot* 62(5): 1581–1591.
32. Yu F, et al. (2010) ANK6, a mitochondrial ankyrin repeat protein, is required for male-female gamete recognition in *Arabidopsis thaliana*. *Proc Natl Acad Sci USA* 107(51): 22332–22337.
33. Lee LY, Fang MJ, Kuang LY, Gelvin SB (2008) Vectors for multi-color bimolecular fluorescence complementation to investigate protein-protein interactions in living plant cells. *Plant Methods* 4:24.
34. Kong L, et al. (2015) Degradation of the ABA co-receptor ABI1 by PUB12/13 U-box E3 ligases. *Nat Commun* 6:8630.
35. Rubio S, et al. (2009) Triple loss of function of protein phosphatases type 2C leads to partial constitutive response to endogenous abscisic acid. *Plant Physiol* 150(3): 1345–1355.

Supporting Information

Chen et al. 10.1073/pnas.1608449113

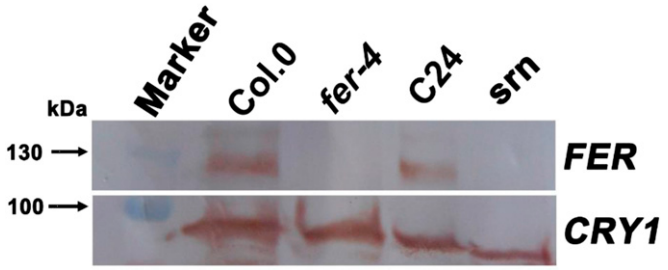

Fig. S1. Specificity analysis of FER antibody. Rosette leaves of 3-wk-old Col.0, *fer-4*, C24, and *srn* mutant plants were harvested, and the total protein was analyzed in a Western blot using FER antibody. CRY1 protein was used as a loading control.

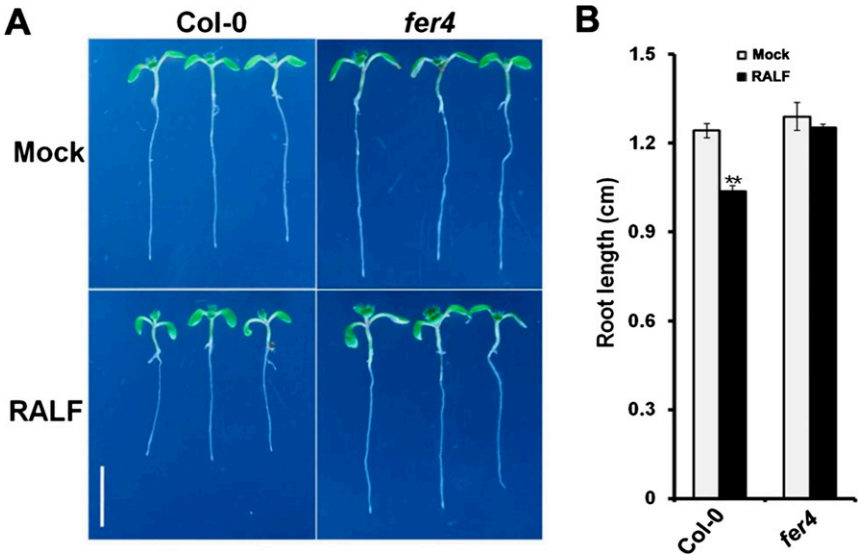

Fig. S2. RALF activity assays. WT, and *fer4* mutant seedlings were treated with 1 μM RALF peptide. Photos were taken (*A*) and root length was measured (*B*) after 3-d treatments. Data in *B* represent average ± SD.

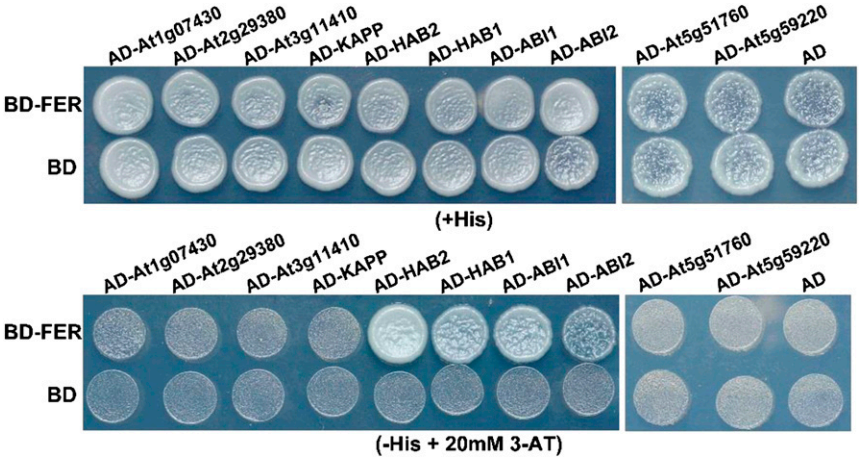

Fig. S3. The interaction analysis between FER and PP2C subfamily members in Y2H. KAPP and PP2CA subfamily members were cloned into the AD vector; FER was cloned into the BD vector. Cells were grown on medium with (*Upper*) or without (*Lower*) His.

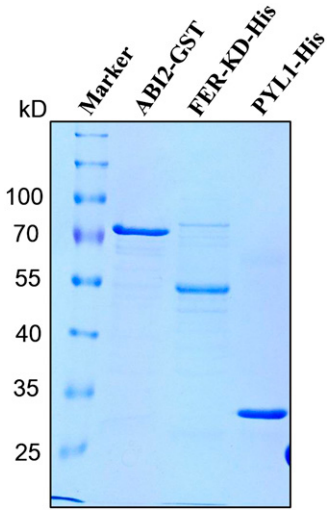

Fig. S4. Purification of proteins. FER-KD-His, ABI2-GST, and PYL1-His was purified and analyzed using SDS/PAGE and Coomassie Brilliant Blue (CBB) staining.

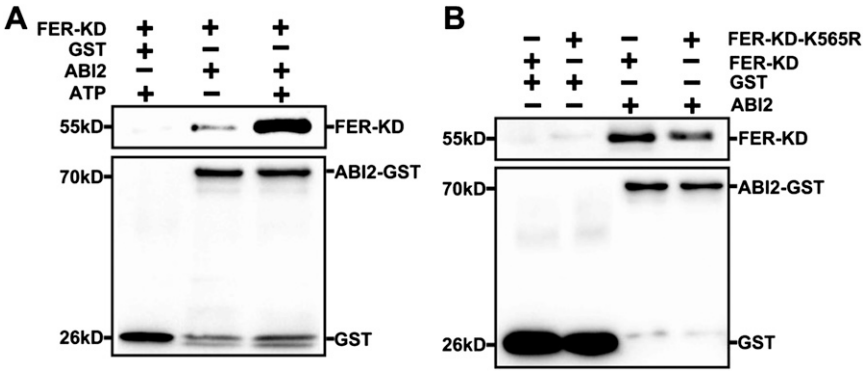

Fig. S5. The ABI2-FER interaction in pull-down assays. (*A*) GST or GST-ABI2 protein was bound to beads and then incubated with His-FER-KD. The eluted proteins were separated by SDS/PAGE and probed with anti-His (*Upper*) or anti-GST antibody (*Lower*). Image is one representative of triplicated experiments showing similar results. (*B*) GST or GST-ABI2 protein was bound to beads and then incubated with His-FER-KD or His-FER-KD-K565R, and the assay was performed as in *A*.

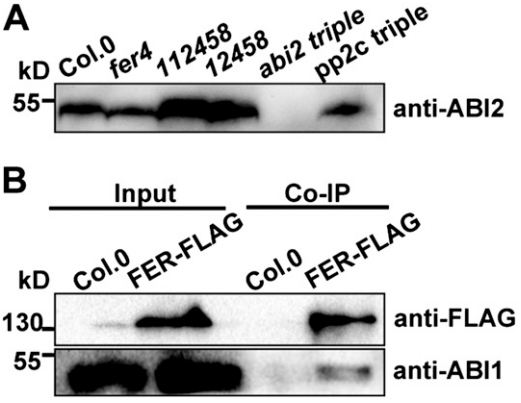

Fig. S6. The interaction of ABI1 with FER-FLAG was detected by Co-IP assay. (*A*) Specificity analysis of anti-ABI2 antibody. Ten-day-old Col.0, *fer4*, *12458*, *112458*, *abi2-2abi1-2hab1-1*(*abi2 triple*), and *abi1-2hab1-1pp2ca-1*(*pp2ca triple*) mutant seedlings were harvested, and the total protein was analyzed in a Western blot, using anti-ABI2 antibody. (*B*) ABI1 interacted with FER-FLAG in vivo. Seven-day-old *Ubi*::FER-FLAG transgenic and Col.0 seedlings were harvested, and total protein was extracted in Co-IP extraction buffer for Western blot analysis, as in ABI2 Co-IP. Three independent experiments were conducted, showing similar results, and one representative blot is shown.

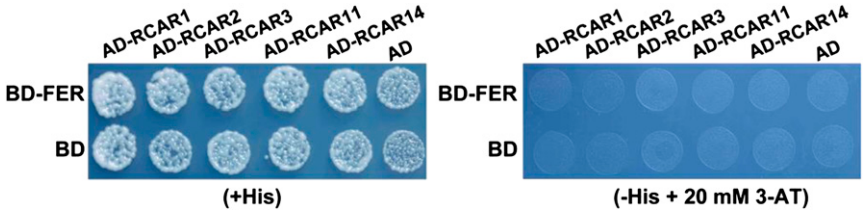

Fig. S7. The interaction analysis between FER and ABA receptor RCARs in Y2H. RCARs were cloned into the AD vector; FER was cloned into the BD vector. Cells were grown on medium with (*Left*) or without (*Right*) His.

Table S1. List of primers

Name	Primer sequence
FERY2HF	5-CGAATTCGCTTACCGCAGACGTAAGC-3
FERY2HR	5-GCTGCAGCTAACGTCCCTTTGGATTCATG-3
FER-BIFCF	5-CGAGCTCGAAGATCACAGAGGGACGATTCC-3
FER-BIFCR	5-TGGATCCAACGTCCCTTTGGATTCATGATCTG-3
FERR-GSTF	5-CGAATTCATGAAGATCACAGAGGGACGATTCC-3
FERR-GSTR	ACTCGAGCGTATTGCTTTTCGATTTCCTAGTAG
ABI2-1 dcapsF	5-CATCATCTGCTATGGCAGG-3
ABI2-1 dcapsR	5-CCGGAGCATGAGCCACAG-3
ABI2Y2HF	5- CAGAATTCATGGACGAAGTTTCTCCTGCAGTC -3
ABI2Y2HR	5- ACGAGCTCTCAATTCAAGGATTTGCTCTTGA-3
ABI2BIFCF	5- ACAGATCTTGGACGAAGTTTCTCCTGCAG-3
ABI2BIFCR	5- CAGAATTCATTCAAGGATTTGCTCTTGA-3
FER-kinase-F	TCACGAATTCCGTGGTGATTACCAGCCTGC
FER-kinase-R	CTGAGTCGACGTCCCTTTGGATTCATG